

Large-signal capabilities of an optically injection-locked semiconductor laser using gain lever

J.-M. Sarraute^{a,b*}, K. Schires^a, S. LaRochelle^b, and F. Grillot^{a,c}

^aLTCl, Télécom Paristech, Université Paris-Saclay, 46 rue Barrault, 75013 Paris, France

^bCOPL, Université Laval, 2375 rue de la Terrasse, Québec Qc, G1V 0A6, Canada

^cCenter for High Technology Materials, University of New-Mexico, 1313 Goddard SE, Albuquerque, NM, United States

ABSTRACT

Directly-modulated lasers remain excellent candidates for the development of efficient and low-cost short reach communication links. While the modulation bandwidth of semiconductor lasers is inherently limited by the relaxation oscillations due carrier-photon interaction, it is possible to further enhance the modulation dynamics by using nonlinear architectures. Our recent studies have revealed the high potential of the optically injection-locked semiconductor laser operating under gain lever effect. Modulation bandwidth as large as 85 GHz, which is namely four times larger than that of the free-running semiconductor laser has been unveiled. In this work, we numerically investigate the large-signal capabilities of this transmitter by evaluating eye diagrams and bit error rates. The results confirm its high potential for short reach communication links operating at high-speeds.

Keywords: Semiconductor laser, injection-locking, gain lever, high-speed communications

1. INTRODUCTION

Development of ultrafast transmitters operating at speeds exceeding 100 Gbps is of paramount importance for increasing the transmission capacity of fiber-based networks, hence directly impacting 5G wireless networks, local and metropolitan area networks as well as long-haul backbones.¹ Although complex modulation formats combined with digital signal post-processing are usually preferred to reach ultra-high modulation bandwidth, the latency introduced by electronic processing results in a severe communication bottleneck. To this end, direct-detection systems implemented with directly modulated lasers remain preferred to improve the high-speed performance and capacity of short reach optical networks (metro, access and data centers).

The 3-dB modulation bandwidth of a directly modulated laser is the most important figure-of-merit determining the maximum bite rate achievable. To keep increasing the bit rate, the enhancement of the 3-dB modulation bandwidth without causing other impairments is highly desired. Such improvements are usually obtained either from the development of novel in-plane semiconductor materials or from the integration of nonlinear architectures such as those using gain lever (GL) and optical injection-locking (OIL).^{2,3} The GL laser is traditionally a semiconductor laser with a short modulation section and a very long one biased under continuous wave (CW) regime near the gain saturation. In order to maximize the GL effect, the modulation section is operated close to the optical transparency e.g. at a point exhibiting high differential gain that transfers the modulation into the long gain section hence improving the modulation dynamics of the whole laser structure. To further improve the high-speed properties, this work investigates the case where the GL laser is optically coupled to an external

*jean-maxime.sarraute.1@ulaval.ca

master laser (ML). When the strength of the injected light and the frequency detuning between the two lasers fall within a certain range and injection-locking is obtained, an ultra large modulation bandwidth well beyond the relaxation oscillation frequency (ROF) of the free-running laser takes place. Therefore, the optical injection-locked gain lever laser (OILGL) constitutes a meaningful solution where the drawbacks of OIL and GL balance each other.⁴⁻⁶ Indeed, while the sole GL produces an increase of the modulation bandwidth,³ it usually comes with a relatively large resonance of the modulation characteristic that is not always desired for practical applications. On the other hand, when a semiconductor laser is purely injection-locked, a large bandwidth enhancement is reached but at the price of a severe frequency dip arising in the modulation response.⁷ Very recently, we have revealed that our OILGL can produce modulation bandwidth as large as 85GHz namely four times larger than that of the free-running semiconductor laser. Besides, unlike any directly modulated semiconductor lasers, the compression factor originating from gain nonlinearities does not affect the OILGL dynamical performance and can even be used to further control the modulation response flatness.⁸ In this work, we go a step beyond by investigating the large-signal capabilities of the OILGL laser through eye diagrams and bit error rates. Overall, the results confirm the great potential of the OILGL for communication links operating at high-speeds.

2. DEVICE DESCRIPTION AND NUMERICAL MODEL

Fig. 1(a) shows schematically the OILGL laser that is composed of two sections electrically isolated but sharing the same active gain medium. The first section ((a)) is very short and pumped close to the optical transparency with $I_a + I_{RF}$ as shown in Fig. 1(a) representing the evolution of the material gain as a function of the carrier density. In order to ensure the GL effect, I_a is chosen such that the steady-state optical gain of section (a) ($G_{a,0}$) remains close to zero. Section (b) is CW-pumped well above the lasing threshold hence the steady-state optical gain ($G_{b,0}$) is near the threshold value (G_{th}). In order to increase the GL dynamics, the parameter h representing the fractional length of section (b) is kept close to the unity. The large difference between the differential gains of each section ($G'_a \gg G'_b$) leads to a significant change of the carrier density in the section (b) while requiring only a small variation of current in the modulation section (a). Fig. 1(b) depicts schematically the OILGL effect. The light output from the ML is injected into the GL laser cavity. The two relevant parameters for the OILGL are the frequency detuning between the two lasers $\Delta f = f_{ML} - f_{GL}$, where $f_{(M/G)L}$ is the lasing frequency of the ML or GL as well as the injected power into the GL cavity P_{ML} .

The dynamics of the OILGL is studied via a rate equation model composed of four differential equations for carriers, photons and phase of the complex field such as:^{4,8,9}

$$\begin{cases} \frac{dN_a}{dt} = \frac{I_a}{eV} - \frac{N_a}{\tau_c} - G_a S, & (1a) \\ \frac{dN_b}{dt} = \frac{I_a}{eV} - \frac{N_b}{\tau_c} - G_b S, & (1b) \\ \frac{dS}{dt} = \left[\Gamma [G_a (1-h) + G_b h] - \frac{1}{\tau_p} \right] S + 2k_c \sqrt{S_{inj}} S \cos(\phi) + R_{sp}, & (1c) \\ \frac{d\phi}{dt} = \left[\Gamma [G_a (1-h) + G_b h] - \frac{1}{\tau_p} \right] \frac{\alpha_H}{2} - \Delta\omega_{inj} - k_c \sqrt{\frac{S_{inj}}{S}} \sin(\phi^0), & (1d) \end{cases}$$

where N_k refers to the carrier density, I_k the current density, τ_c the carrier lifetime and G_k the unclamped material gain of section k . As shown in Eq. 1a and Eq. 1b, τ_c is kept identical for both long and short sections owing to the same active area. As regards the optical injection, S_{inj} is the photon density injected with a coupling

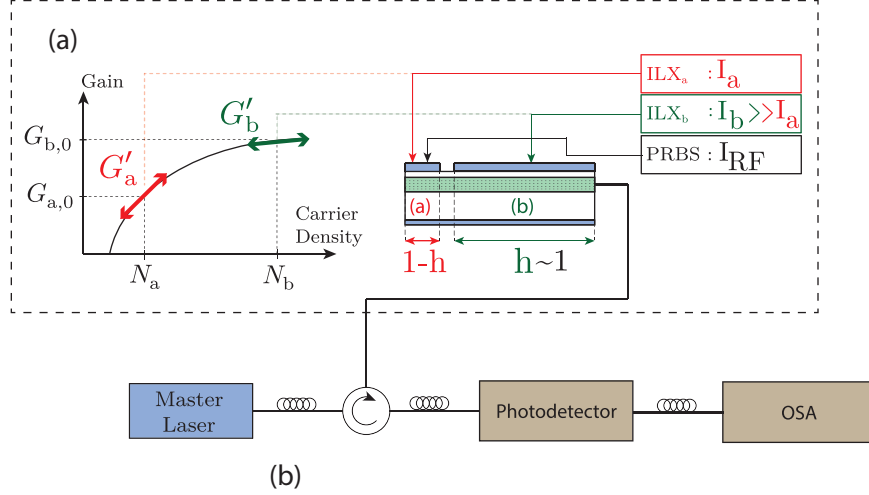


FIG. 1: Schematic view of the OILGL laser. The left figure gives the evolution of the material gain with carrier density and shows the differential gain in both sections

factor efficiency k_c and detuned from the free-running SL by $\Delta\omega_{inj} = 2\pi\Delta f$, with ϕ the phase offset between ML and GL. Finally, S and τ_p are the photon density and photon lifetime of the GL cavity, respectively, while α_H corresponds to the linewidth enhancement factor. Let us recall that h is the fractional length of section (b) while Γ is the optical confinement factor. Spontaneous emission is taken into account with the term R_{sp} in equation (1c) such as $R_{sp} = \Gamma\beta \left[(1-h) \frac{N_a}{\tau_c} + h \frac{N_b}{\tau_c} \right]$ with β the spontaneous emission factor and where each section contributes to spontaneous emission with respect to their length h . According to,² a logarithmic gain is then taken into account and is written:

$$G_k(N_k, S) = \frac{G_{k,0}}{1 + \varepsilon S} \ln \left(\frac{N_k + N_s}{N_{tr} + N_s} \right), \quad (2)$$

where ε is the gain compression factor, N_{tr} the carrier density at transparency, N_s a fitting parameter,² and $G_{k,0}$ the steady-state optical gains.

3. SIMULATION RESULTS

The set of differential rate equations is numerically solved using a Runge-Kutta algorithm incorporating material and laser parameters given in Tab. 1. In order to provide the GL effect, section (b) is operated under CW with $I_{dc,b}$, while the shorter section (a) has both a DC bias current and a (RF) biased such that $I_{dc,a} + I_{RF}$ (with $I_{dc,a} \ll I_{dc,b}$). Let us stress that the modulated part of the current applied onto section (b) depends on the PRBS peak-to-peak voltage U_{P2P} . The values of I_{mod} for "0" ($I_{mod,0}$) and "1" ($I_{mod,1}$) have been fixed to experimentally reasonable values: $I_{mod,0} = -0.252 \times I_{th}$ and $I_{mod,1} = 0.253 \times I_{th}$. In what follows, the rate equations are numerically solved under large-signals assuming a pseudo-random bit sequence (PRBS) of pattern length of 5,000 bits. Two bit rates are considered namely $B = 2.5$ Gbps and $B = 5$ Gbps.

Back-to-back configuration

First, eye diagrams of the free running laser characteristics operating without optical injection and GL are computed. In Fig. 2, simulations are performed using $U_{P2P} = 450$ mV, $h = 0.5$ and $I_{dc,a} = I_{dc,b} = 3 \times I_{th}$. Whatever the bit rate, the free-running configuration provides opened eye diagrams with an optical modulation

Table 1: Material and laser parameters used in the simulations

Simulation parameters	Symbols	Value
Cavity length	L	500×10^{-6} m
Mirror reflectivity	$R_1 = R_2$	0.32
Threshold current	I_{th}	6.58 mA
modulated current for a "0" (section b)	$I_{mod,0}$	$-0.252 \times I_{th}$
modulated current for a "1" (section b)	$I_{mod,1}$	$0.253 \times I_{th}$
Steady-state optical gain (section b)	$G_{b,0}$	1.8×10^{13} s ⁻¹
Optical index	n_g	3.5
Carrier lifetime	τ_c	0.1×10^{-9} s
Photon lifetime	τ_p	3.17×10^{-12} s
Linewidth enhancement Factor	α_H	2
Coupling S-M factor	k_c	1×10^{11} s ⁻¹
Gain Compression factor (section b)	ε	5×10^{-17} cm ³
Optical confinement	Γ	0.03
Spontaneous emission factor	β	10^{-5}

amplitude OMA ($OMA \triangleq (P_1 - P_0)/P_0$, with $P_{1/0}$ the output power for a "1"/"0") around 0.3 both at 2.5 Gbps and 5 Gbps. However, some overshoots attributed to the relaxation oscillations and the low damping factor of the laser are observed in the eye diagrams.

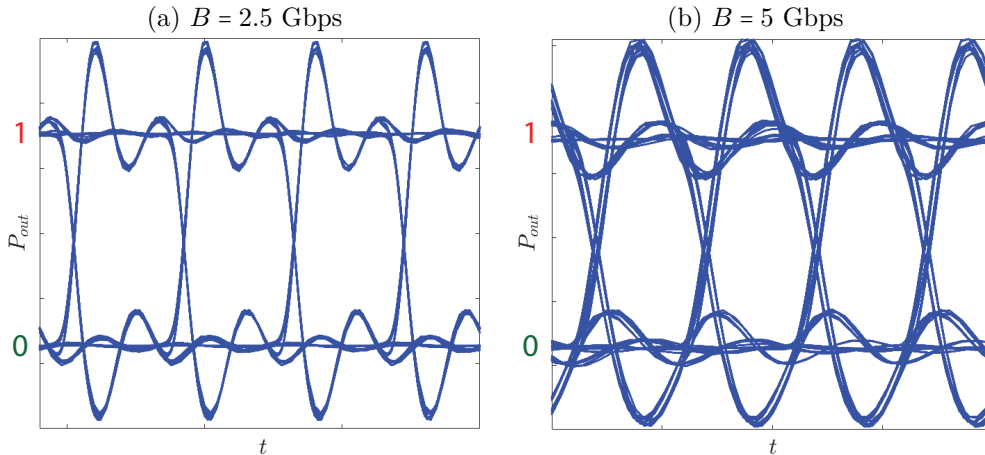


FIG. 2: Computed eye diagrams for the free running laser (direct modulation) operating without GL and OIL with $U_{P2P} = 450$ mV, $I_{DC} = 3 \times I_{th}$ for (a) $B = 2.5$ Gbps and (b) $B = 5$ Gbps. Other parameters are given in Tab. 1

Then, the effect of the sole OIL on the high-speed capabilities is investigated. As the stable-locking area is located between the saddle-node (SN) and the Hopf (H) bifurcations,⁹ the frequency detuning Δf is chosen with respect to the injection strength K such that :

$$\Delta f \triangleq \frac{1}{4} (\text{SN}(K) + 3 \times \text{H}(K)) \quad (3)$$

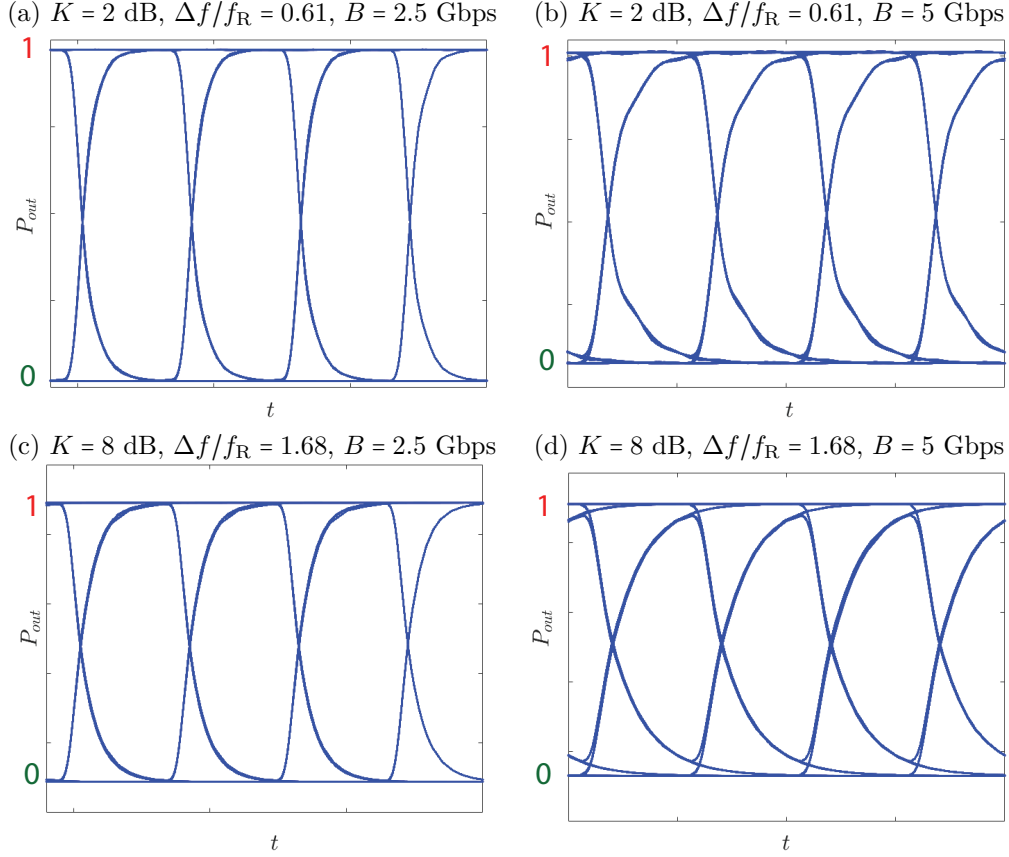


FIG. 3: Computed eye diagrams for an OIL laser (direct modulation) with ($K = 2$ dB, $\Delta f = 0.61 \times f_R$) for (a) $B = 2.5$ Gbps and (b) $B = 5$ Gbps and with ($K = 8$ dB, $\Delta f = 1.68 \times f_R$) for (c) $B = 2.5$ Gbps and (d) $B = 5$ Gbps. Other parameters are given in Tab. 1

In Fig. 3 eye diagrams of an OIL directly modulated laser is calculated for two values of the optical injection parameters ($K, \Delta f$). Simulations are obtained assuming the same conditions as for the free-running case. Fig. 3 (a) and (b) shows the eye diagrams computed for lower injection case with $K = 2$ dB and frequency detuning of $\Delta f = 0.61 \times f_R$ while Fig. 3(c) and (d) unveils the case for stronger injection with $K = 8$ dB and $\Delta f = 1.68 \times f_R$. Eye diagrams are perfectly opened for both low and high injection strengths show that, overshoots due to the transient chirp are fully suppressed. However, as aforementioned, strong injection of light always leads to a frequency dip in the modulation response hence shrinking the high-speed capabilities of such lasers to very narrow window of operation. In addition to that, simulations show that optical injection increases output power levels of "0" and "1".

Next step consists in studying the effect of the sole GL on the transmission capabilities. As detailed on,^{5,6} the strength of the GL is mostly driven by the physical quantity g corresponding to the ratio between the damping factors of section (a) γ_a to that of section (b) γ_b ($g \doteq \gamma_a/\gamma_b$). On the first hand, using $h = 0.8$ with bias conditions such as $I_{dc,a} = 0.4 \times I_{th}$ and $I_{dc,b}/I_{dc,a} = 15$ leads to a value of g of about 3. A higher g close to 10 can be obtained by decreasing $I_{dc,a}$ down to $0.2 \times I_{th}$ and taking $I_{dc,b}/I_{dc,a} = 40$. Fig. 4 depicts the eye diagrams for the GL directly modulated laser operating without optical injection for $g = 3$ and $g = 10$. As shown in 4, the activation of the GL increases both the output powers of "0" and "1" as well as the overshoots generated by bit transitions

which is consistent since the sole GL effect increases the modulation efficiency. Simulations also reveal that eye diagrams at 5 Gbps are more opened than those at 2.5 Gbps meaning that a high value of g produces a wider the modulation bandwidth. Fig. 5 now depicts the simulations for the OILGL with $g = 10$ ($I_{dc,a} = 0.22 \times I_{th}$,

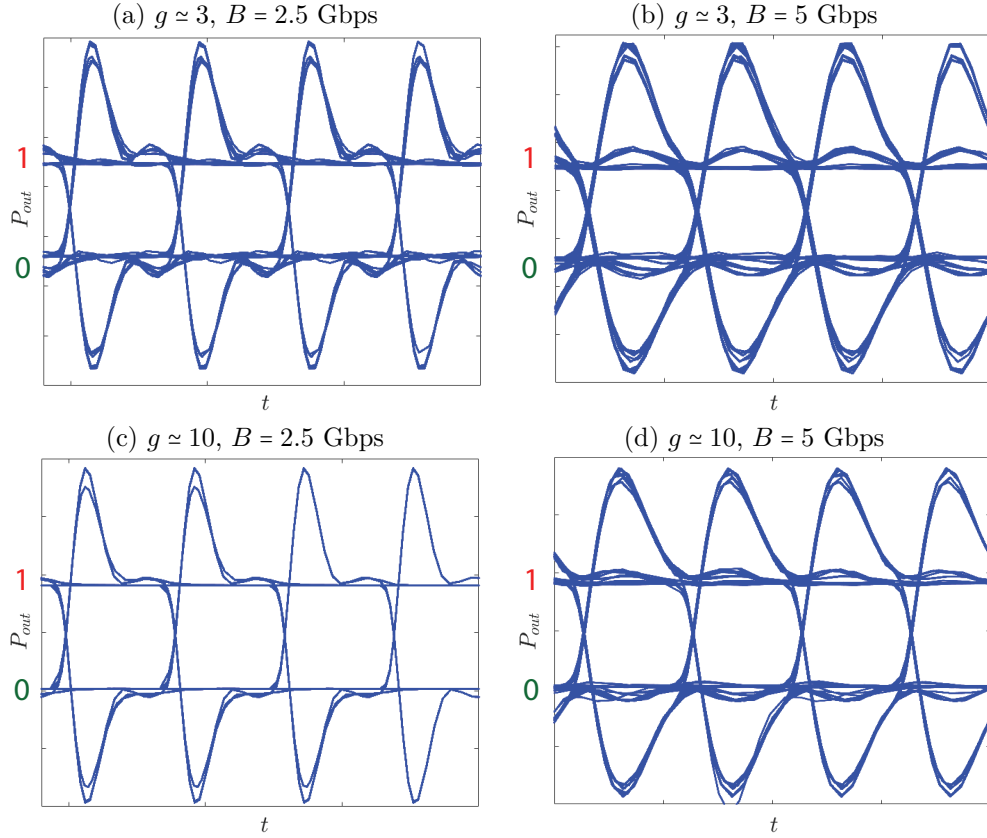


FIG. 4: Computed eye diagrams for a GL laser (direct modulation) with $g = 3$ for (a) $B = 2.5$ Gbps and (b) $B = 5$ Gbps and with $g = 10$ for (c) $B = 2.5$ Gbps and (d) $B = 5$ Gbps. Other parameters are given in Tab. 1

$I_{dc,b}/I_{dc,a} = 40$, and $h = 0.8$). Injection parameters are $K = 8$ dB and $\Delta f = 1.68 \times f_R$. As discussed in,⁶ those conditions correspond to an achievable 3-dB bandwidth close to 85 GHz. For this set of parameters ($h, g, K, \Delta f$) and those given in Tab. 1, eye diagrams are computed and reported in Fig. 5(a) for $B = 10$ Gbps, Fig. 5(b) for $B = 20$ Gbps, Fig. 5(c) for $B = 30$ Gbps and finally in Fig. 5(d) for $B = 40$ Gbps. As shown, the OILGL exhibits faster speeds which proves that the drawbacks of the OIL and GL are balanced each other. Overall, simulations demonstrate high-speed capabilities up to 40 Gbps with clear opened eyes (Fig. 5(d)) and no overshoots. In order to better underpin the capabilities of the OILGL for high-speed operation, Fig. 6 provides the evolution of the bit error rate (BER) with respect to the bit rate for $h = 8$, $g = 10$ and $(K, \Delta f/f_R) = (8, 1.62)$. The BER is the number of bit errors divided by the total number of transferred bits during a studied time interval. In the optical communication system, the BER may be affected by transmission channel noise, interference, distortion, bit synchronization problems, attenuation, and spectral instabilities. The calculation of the BER takes into account both shot and thermal noises. As illustrated, BER is a about 10^{-4} for $B = 10$ Gbps and increases until 10^{-2} for $B = 40$ Gbps. Note that in this work, the BER is computed without any digital signal processing and may be further improved using error correcting code.

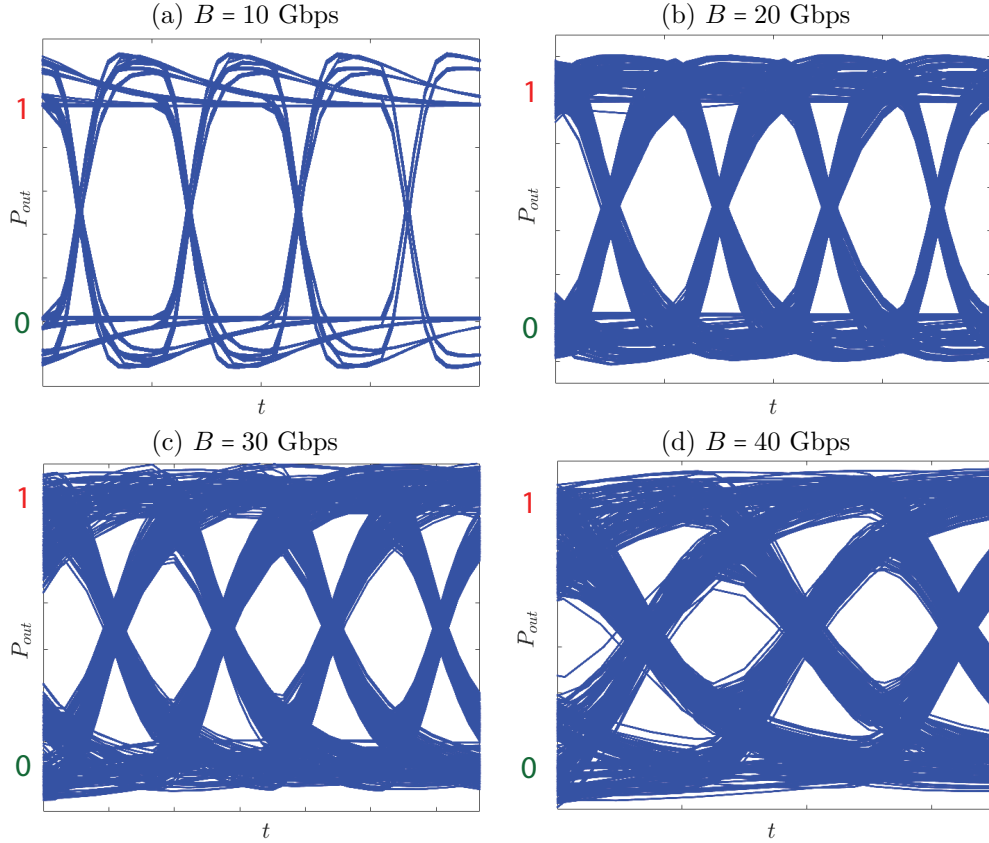


FIG. 5: Computed eye diagrams for the OILGL (direct modulation) with $g = 10$, $K = 2$ dB, $\Delta f = 0.61 \times f_R$ for (a) $B = 10$ Gbps, (b) $B = 20$ Gbps, (c) $B = 30$ Gbps and (d) $B = 40$ Gbps. Other parameters are given in Tab. 1

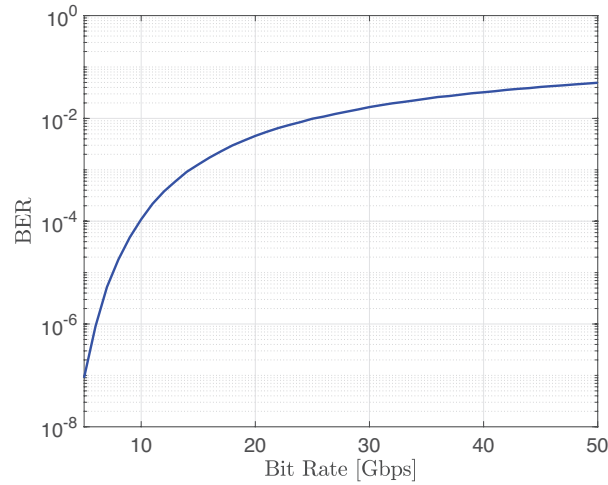


FIG. 6: BER for the OILGL with respect to the bit rate for $g = 10$ and $(K, \Delta f/f_R) = (8, 1.62)$

Transmission configuration

Finally, we investigate the impact of the chromatic dispersion due to signal propagation across an optical fiber taking a chromatic dispersion coefficient of 18 ps/(km.nm) and an attenuation coefficient of 0.2 dB/km at

$\lambda = 1550$ nm. Fig. 7 illustrates the OILGL eye diagrams for $h = 0.8$, $g = 10$, $K = 8$ dB and $\Delta f/f_R = 1.68$ and $B=20$ Gbps assuming propagation distances of 5 and 10 km respectively which is in compliance with short reach requirements. Results confirm that eye diagrams remain slightly affected by the transmission distance. The BER extracted from the eyes diagrams are similar to those obtained for the back-to-back configuration with values around 1.1×10^{-4} after 5 km propagation distance and 1.3×10^{-4} after 10 km respectively.

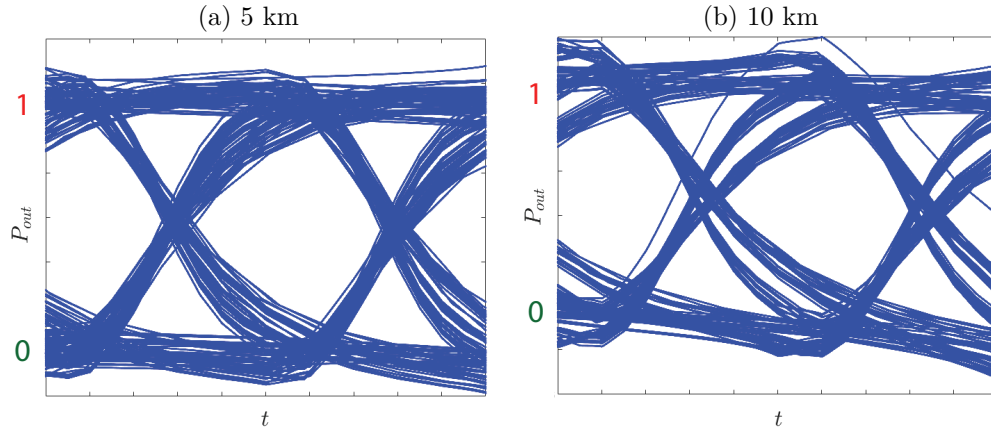


FIG. 7: Computed eye diagrams for the OILGL (direct modulation) and chromatic dispersion coefficient $\beta_2 = 18\text{ps}/(\text{km}\cdot\text{nm})$ for $g = 10$, $K = 8$ dB, $\Delta f = 0.61 \times f_R$ and $B = 20$ Gbps for fiber length of (a) 5 km and (b) 10 km

4. CONCLUSIONS

To sum, this paper investigates the potential of the OILGL semiconductor laser on transmission capabilities. By using a Runge-Kutta algorithm, the rate equations are numerically solved under large-signals. Calculations confirm the great potential of using the OILGL for high-speed applications. Considering a strong optical injection case combined with a high GL leads to a 40 Gbps direct modulation operation with clear opened eye involved by the flatness of the modulation response. After propagation, the BER extracted at 20 Gbps is similar to that obtained for the back-to-back configuration which can be further improved with an error correcting code. Consequently, future work will also consider longer bit sequences to evaluate the full performance of the OILGL. These results give selection rules for designing novel high-speed transmitters compatible with future short communication link requirements.

ACKNOWLEDGMENTS

This work is supported by the Institut Mines-Télécom as well as by the NSERC through the CRC in Advanced Photonics Technologies for Communications

REFERENCES

- [1] Yamamoto, T., “High-speed directly modulated lasers,” in [Optical Fiber Communication Conference (paper OTh3F)], 225–228 (March (2012)).
- [2] Coldren, L. and Corzine, S., [Diode Lasers and Photonic Integrated Circuits], Wiley Series in Microwave and Optical Engineering, Wiley (1995).
- [3] Vahala, K., Newkirk, M. A., and Chen, T., “The optical gain lever: A novel gain mechanism in the direct modulation of quantum well semiconductor lasers,” Applied Physics Letters **54**, 2506–2508 (June (1989)).
- [4] Sarraute, J. M., Schires, K., LaRochelle, S., and Grillot, F., “Enhancement of the modulation dynamics of an optically injection-locked semiconductor laser using gain lever,” Journal of Selected Topics in Quantum Electronics, IEEE **21**, 1801408 (November/December (2015)).
- [5] Sarraute, J.-M., Schires, K., LaRochelle, S., and Grillot, F., “Gain compression effect on the modulation dynamics of an optically injection-locked semiconductor laser using gain lever,” in [SPIE OPTO], 97420E–97420E, International Society for Optics and Photonics (2016).
- [6] Sarraute, J., Schires, K., LaRochelle, S., and Grillot, F., “Effects of gain nonlinearities in an optically injected gain lever semiconductor laser,” Photonics Research **5**(4), 315–319 (2017).
- [7] Simpson, T. B., Liu, J., and Gavrielides, A., “Bandwidth enhancement and broadband noise reduction in injection-locked semiconductor lasers,” Photonics Technology Letters, IEEE **7**, 709–711 (July (1995)).
- [8] Sarraute, J., Schires, K., LaRochelle, S., and Grillot, F., “Effects of gain nonlinearities in an optically injected gain lever semiconductor laser,” Photonics Research **5**(4), 315–319 (2017).
- [9] Sarraute, J.-M., Schires, K., LaRochelle, S., and Grillot, F., “Gain compression effect on the modulation dynamics of an optically injection-locked semiconductor laser using gain lever,” in [Physics and Simulation of Optoelectronic Devices XXIV], **9742**, 97420E, International Society for Optics and Photonics (2016).